July 24, 2003

Ken Zweibel
National Renewable Energy Laboratory
1617 Cole Boulevard
Golden, CO 80401

Re: NREL Subcontract #ADJ-1-30630-12

Dear Ken:

This report covers research conducted at the Institute of Energy Conversion (IEC) for the period
June 03, 2003 to July 03, 2003, under the subject subcontract. The report highlights progress and
results obtained under Task 3 (Si-based Solar Cells) and Task 4 (Diagnostics).

Task 3: Si-based Solar Cells

In order to develop thin film Si devices, the focus of this task has shifted to the development of
doped films. In this period, Boron doped HWCVD films were deposited and characterized. The
deposition conditions used are summarized in Table 3.1.

Table 3.1. B-doped Si film deposition conditions.

Substrate temperature (°C)	450
Wire temperature (°C)	1850
Pressure (mTorr)	200
SiH_4 flow (sccm)	4.0
B_2H_6/SiH_4	$10^{-5} - 10^{-3}$
Deposition time (min)	30

In addition, a set of undoped films was also deposited for comparison. For these films, the
deposition conditions were similar as in Table 3.1, except that an additional 2 sccm of H_2 was

added to the gas mixture to make up for the H_2 diluent in the B_2H_6 dopant mixture. The film thickness for all films varied from 0.56 to 0.73 µm. XRD and Raman spectroscopy analysis, as seen in Figures 3.1 and 3.2 for a representative sample, shows that the films are highly crystalline and exhibit typical (220) preferential orientation. Calculation of the crystalline fraction from the Raman profiles results in values from 75 to 90%.
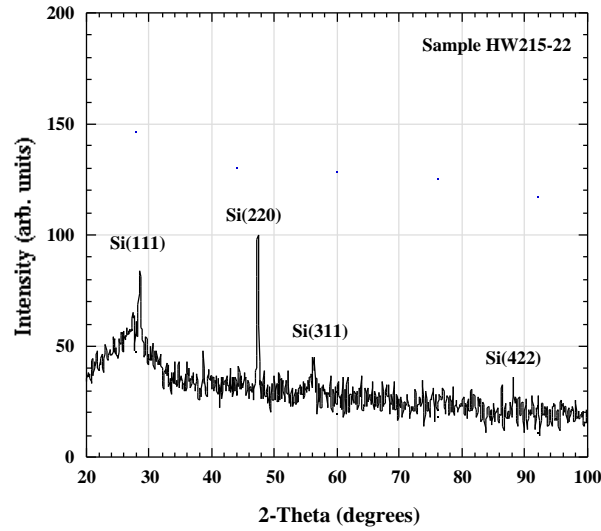

Figure 3.1. XRD pattern of B-doped HWCVD µc-Si film.

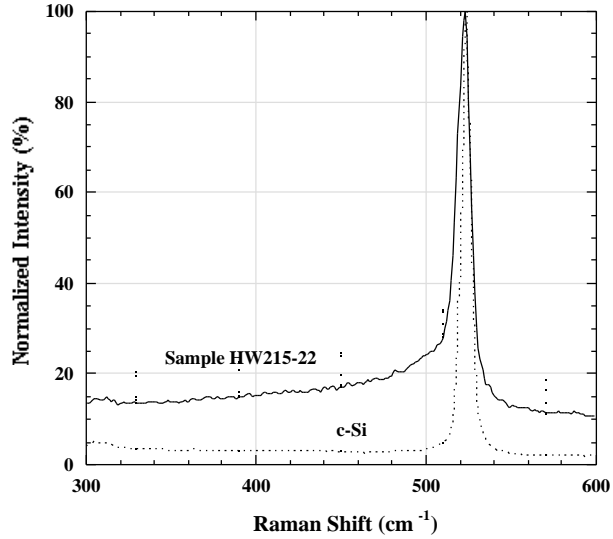
Figure 3.2. Raman spectra of B-doped HWCVD µc-Si film.

Values of the room temperature light and dark conductivity measured by the 4-point probe method, as a function of the B_2H_6/SiH_4 in the gas phase are summarized in Table 3.2. The

invariance of conductivity with dopant gas concentration indicates poor incorporation of B from the gas phase at the conditions used. Previous experiments carried out at P = 500 mTorr and $B_2H_6/SiH_4 = 1x10^{-3}$ with other parameters similar to those in Table 3.1 yielded films with conductivities of $\sim 10^{-1}$ S/cm. However, the films had a significant thickness gradient along the direction of flow, due to the high pressure. A pressure of 200 mTorr was used for this study to achieve greater uniformity. The effects of deposition parameters on the decomposition of B_2H_6 and the incorporation of Boron in HWCVD Si films have not been studied as extensively as those for SiH_4. Thus, in the next period, growth conditions will be optimized to achieve reasonable thickness uniformity and film conductivities in the range suitable for devices.

Table 3.2. Conductivity of B-doped Si films.

Sample #	B_2H_6/SiH_4	Dark Cond. (S/cm)	Light Cond. (S/cm)
HW212-21	0	$1.1x10^{-6}$	$1.6x10^{-6}$
HW215-21	$1x10^{-5}$	$3.5x10^{-6}$	$2.0x10^{-6}$
HW216-21	$1x10^{-4}$	$2.4x10^{-6}$	$2.3x10^{-6}$
HW217-21	$1x10^{-3}$	$1.7x10^{-6}$	$1.8x10^{-6}$

In the area of grain size enhancement of Si films, aluminum-induced crystallization (AIC) experiments of a-Si films deposited by PVD methods have been performed to compare the effects of the in-situ AIC and standard AIC process on film properties and grain enhancement mechanism. Two key differences between the approaches to be examined are the presence of an atomic hydrogen atmosphere and the dynamic nature of the crystallization/enhancement mechanism in the in-situ AIC process compared to the standard process. In this period, thin Si films have been deposited by sputtering and electron beam evaporation onto 500 nm Al layers deposited also by either sputtering or electron beam evaporation. The stack layer structures were subsequently annealed in a tube furnace under Ar flow of 100 sccm at 1 Atm pressure. Annealing was carried out at 400° and 600 ^{0}C for 45 minutes, followed by either quenching or slow cooling profiles. Further details on the experiments and film characterization will be reported in the next quarter.

Task 4: Diagnostics

Contact wetting angle measurements of water on CdTe films at different stages of processing are correlated with surface phase composition. Additionally, polar and dispersive components of the surface energy on Cu(InGa)Se$_2$ films with different composition are evaluated. Reduction techniques were refined to facilitate reduction of contact angle measurements using multiple liquids to separate polar and dispersive components of surface energy.

For measurement of the wettability of liquid on a solid surface, a useful comparative quantity is the adhesive energy, E_{ad}, expressed in terms of the liquid surface tension and the contact angle:

(1) $E_{ad} = E_{LV}(1 + \cos\ )$

As the wettability of a liquid on a solid surface *decreases*, the contact angle increases, $\theta \to 90$, $cos(\theta) \to 0$, and $E_{ad} \to E_{LV}$. In this case, the adhesive energy approaches the surface tension at the liquid-vapor interface. As the wettability further decreases, $\theta > 90$, and $cos(\theta) < 0$. In this case the adhesive energy is less than the liquid-vapor energy and the droplet will be poorly adhered to the surface. As the wettability *increases*, the contact angle decreases, $\theta \to 0$, $cos(\theta) \to 1$, and $E_{ad} > E_{LV}$.

Vapor transport CdTe films supplied by First Solar as part of team activity were analyzed by glancing incidence x-ray diffraction (GIXRD) and contact angle at different stages of post-deposition processing. The GIXRD measurements were made on a Rigaku D/Max 2500 instrument with Cukα x-rays at 40 kV and 50 mA, with incident beam angle at 0.5°, sampling an average depth of ~60 nm. The contact angle measurements of deionized water drops on the CdTe surface were carried out at room temperature (20°-25°C) and pressure using a horizontal microscope at ~20X, fitted with a protractor reticle and *x-y-z* motion stage. The contact angle was determined with a precision of ±2°. For each sample, the contact angle of the left and right side of 6 different drops were measured and the average taken. Each drop has a volume of ~0.05 cm^3 and was dispensed from a capillary pipette situated 2 cm above the level film specimen. Prior to measuring the contact angle, each drop was allowed to reach equilibrium with the surface for >10 s. The films were rinsed in isopropanol (IPA) and dried under argon prior to contact angle measurement.

The GIXRD and contact angle data are listed in Table 4.1. For as-received vapor transport CdTe films, only the CdTe phase was found and the contact angle was typically >70°. Annealling the film in dry air at 600°C, with water concentration less than 0.01 mg/L, caused insignificant change in surface properties. Performing a CdCl$_2$ vapor treatment at 430°C in dry air produced a CdO phase, detectable after 30 minutes of treatment, as has been reported in previous studies[i]. However, an increase in wetting was detected after only 15 minutes. Similar adhesion was found for both 15 and 30 minute treatments, suggesting that the CdO phase is present in both cases, but is thinner than the GIXRD detection limit for the 15 minute case. For CdCl$_2$ treatment carried out in moist room air, with water concentration ~0.01 g/L, the native oxides CdTeO$_3$ and CdTe$_2$O$_5$ were found, and no CdO was detected. The proportion of CdTe$_2$O$_5$ increased with time, further reducing the adhesion. For the sample vapor CdCl$_2$ treated in dry air, the three-step BDH etch was used to produce a Te layer, as shown by the GIXRD result. This significantly reduced the wetting. After 30 minutes resting in room air, re-rinsed with IPA, and analyzed, the wetting increased, suggesting the formation of Te oxides too thin for GIXRD detection. This result is qualitatively similar to that reported earlier for ellipsometric changes on Te surfaces produced by NP etching[ii]. These relative measurements provide a sensitive means to monitor changes in CdTe surface condition.

Table 4.1. GIXRD and contact angle results for CdTe surfaces at different stages of post-deposition processing. Samples marked with (*) are the same specimen.

Processing Stage	Conditions	Surface Phases from GIXRD	Contact Angle for H_2O (±2 degrees)	Adhesive Energy for H_2O (±2 dyn/cm)
As -Received		CdTe	80	86
Dry Air Anneal	600C, 20 min	+ $CdTeO_3$	70	98
$CdCl_2$+Dry Air	430C, 15 min	CdTe	30	136
*$CdCl_2$+Dry Air	430C, 30 min	+ CdO	25	140
$CdCl_2$+Moist Air	430C, 15 min	+ $CdTeO_3$	35	132
$CdCl_2$+Moist Air	430C, 30 min	+ $CdTeO_3$, $CdTe_2O_5$	45	124
$CdCl_2$+Moist Air	430C, 60 min	+ $CdTeO_3$, $CdTe_2O_5$	55	114
*BDH etch	immediately	Te	60	110
*BDH etch	0.5 hr after	Te	40	130

The Zisman method discussed in the previous report for determination of solid-vapor energy has been evaluated for $Cu(InGa)Se_2$ and $(CdZn)Te$ alloys, with the result that the extrapolation method is too inaccurate to achieve a reasonable degree of accuracy or repeatability. This is because the method is best suited for liquids with a low fraction of polar energy. The total free surface energy consists of both polar and London dispersive components:

(2) $E = E^p + E^d$

The components are different for different fluids and can result in non-linear behavior on a Zisman plot of $cos(\ )$ versus E_{LV}. The polar component, E^d, arises from permanent dipoles, induced dipoles and hydrogen bonding. The London dispersion force component of the surface free energy, E^p, arises from interactions between fluctuating electronic dipoles with induced dipoles. A simple *rule of thumb* is that a low energy liquid such as acetophenone will wet and strongly adhere to a high energy solid such as stannic oxide. This rule holds only if the intermolecular forces in both solid and liquid can interact. The rule breaks down, however, when the force interaction is restricted, such as observed for water on oxide-free high-energy metals. In our studies, we intended to utilize water for routine analysis. Thus, a more detailed reduction process was needed.

A more quantitative assessment can be obtained using two or more liquids by the *harmonic mean* method in which the polar and dispersive components of the solid, E_S^p and E_S^d, are determined. For liquid 1, we have $E_1 = E_1^d + E_1^p$ and for liquid 2, $E_2 = E_2^d + E_2^p$:

(3a) $(1 + \cos\ _1)E_1 = 4 \left[\dfrac{E_1^d E_S^d}{E_1^d + E_S^d} + \dfrac{E_1^p E_S^p}{E_1^p + E_S^p} \right]$

(3b) $(1 + \cos\theta_2)E_2 = 4\left[\dfrac{E_2^d E_S^d}{E_2^d + E_S^d} + \dfrac{E_2^p E_S^p}{E_2^p + E_S^p}\right]$

Equations 3a and 3b can be solved simultaneously for the solid surface energy components E_S^p and E_S^d, given the contact angles and corresponding polar and dispersive energies of the two fluids. The polar fraction of the surface energy is represented as x_p. This type of analysis has been carried out on Cu(InGa)Se$_2$ films deposited with similar Cu composition but different Ga content, all with a final thermal step at 550°C (Table 4.2). The average contact angles of water ($x_p = 0.32$) and formamide ($x_p = 0.70$) were determined for the left and right sides of 3 drops, with a precision of ±1°. From the contact angle results, it is apparent that water wets samples with Ga better than samples without, while the wetting of formamide was unaffected by composition. Using the Zisman analysis method, a surface energy of 55 dyn/cm was determined for all samples. However, the results using the *harmonic mean* analysis indicate a similar dispersive component for all samples, but higher polar component for samples with Ga. This preliminary result suggests that the polar component of the surface energy in Cu(InGa)Se$_2$ films may be influenced by Ga concentration. A more detailed study of this dependence will be carried out.

Table 4.2. Contact wetting angle and surface energy for Cu(InGa)Se$_2$ films.

Sample	Cu/(III)	Ga/(III)	water	formamide	E^p (dyn/cm)	E^d (dyn/cm)	E_{SV} (dyn/cm)
33696.21	0.82	0	43	14	29	31	60
33690.21	0.75	0.30	26	13	40	27	67
33708.21	0.77	0.31	18	14	45	25	70

Sincerely,

Robert W. Birkmire
Director

RWB/bj

Cc: Gerri Hobbs
Cc: Carolyn Lopez
Cc: Roger Aparicio
CC: Erten Eser
Cc: Steven Hegedus

---

[i] see, for example, B. E. McCandless, Sym. Proc. MRS, 668 (2001) H1.6.1.
[ii] K. D. Dobson, P. D. Paulson, B. E. McCandless, R. W. Birkmire, Presented at Spring 2003 MRS Conference, San Francisco.